

Carbon monoxide oxidation over CuO/CeO₂ catalysts

Xiaolan Tang, Baocai Zhang, Yong Li, Yide Xu, Qin Xin, Wenjie Shen*

State Key Laboratory of Catalysis, Dalian Institute of Chemical Physics, Chinese Academy of Sciences,
P.O. Box 110, 457 Zhongshan Road, Dalian 116023, China

Available online 6 July 2004

Abstract

CuO/CeO₂ catalysts prepared by co-precipitation, deposition-precipitation and impregnation methods were extensively investigated for CO oxidation reaction. It was shown that the catalytic behaviors of CuO/CeO₂ catalysts greatly depended on the preparation routes, which caused significant differences in the redox properties and the dispersion of copper species. The remarkable redox ability of CuO/CeO₂ at lower temperatures was found to play an essential role in CO oxidation reaction. The catalysts prepared by co-precipitation exhibited the highest catalytic activity in CO oxidation with CO total conversion at 85 °C. The structural characters as well as the redox features of CuO/CeO₂ catalysts were comparatively investigated by XRD, TPR, cyclic voltammetry and XPS measurements. The discrepancies in the dispersion of copper species and the degree of interaction between copper species and ceria determined the reversible redox properties, and consequently the catalytic performance.

© 2004 Elsevier B.V. All rights reserved.

Keywords: CO oxidation; CuO/CeO₂; Redox; Dispersion; Metal–support interaction

1. Introduction

Many recent studies have shown that the activities of ceria-related catalysts in complete oxidation reactions are greatly enhanced not only by precious metals, but also by base metals [1–4]. Among them, copper or copper oxide on ceria is known to be an efficient catalyst for various reactions such as the total oxidations of CO, methanol and methane [4,5]. The role of ceria as a support for base metals is not only related to its oxygen storage capacity, but also to the ability of improving dispersion of the base metals. Ceria provides the unique capability of promoting oxidation reactions, due to its easy generation of oxygen vacancies to form interfacial active centers. As a consequence, the metal–support interaction can be established to explain the high catalytic performance in specific reactions. However, it is not entirely clear how the redox properties and the copper–ceria interaction of CuO/CeO₂ affect the catalytic performance, although the high oxygen storage capacity and facile Ce⁴⁺/Ce³⁺ redox cycle in ceria appear to play significant roles. Controversial conclusions are

often withdrawn probably due to the variations of preparation processes applied in obtaining the catalysts.

The rapid growth in the applications and the characterization of CeO₂-containing catalysts in the past decade has been well documented [6,7]. Particularly, the CuO/CeO₂ catalyst was reported to be very active for the complete CO oxidation, exhibiting a specific activity several orders of magnitude higher than that of conventional Cu-based catalysts and even comparable to precious metals [4]. The high activity of CuO/CeO₂ was attributed to the quick reversible redox process of superficial Cu(I)/(II) couples in a strong synergistic interaction with the nanocrystalline ceria [8]. Both the composition and the nanostructured morphology of CuO_x/CeO₂ were suggested to greatly influence the reaction rate of CO oxidation with the conclusion that easily reducible, high-energy surfaces of CeO₂ are better in stabilizing the highly dispersed copper species by a closed synergistic interaction [8]. The redox properties of ceria and the high mobility of lattice oxygen were generally regarded to play key roles in governing the catalytic behaviors.

The preparation methods have been reported to affect the activity of Cu-reducible oxide system significantly [8]. The variations of the preparation routes often lead to the changes in the morphology and in the dispersion of copper species. Therefore, remarkable discrepancies in the catalytic performance are often observed. The currently employed methods

* Corresponding author. Tel.: +86 411 84379085;
fax: +86 411 84694447.

E-mail address: shen98@dicp.ac.cn (W. Shen).

include co-precipitation [9], deposition-precipitation [10], impregnation [4], used solvates metal atom impregnation [11], inert gas condensation [12] and sol–gel method so on [13]. However, no systematic investigation was carried out to reveal the nature of the catalytic activity caused by different preparation techniques. On the other hand, the redox properties of CuO/CeO₂ catalyst have important influence on catalytic activity for oxidation reactions [14–16]. However, how to improve and control redox properties in preparation process is still a fundamental challenge, which needs detailed understanding of the correlation between redox properties and preparation routes.

The present study is aimed to establish the correlations between preparation routes and catalytic properties. Three commonly applied preparation methods, co-precipitation, deposition-precipitation and impregnation were used to prepare CuO/CeO₂ catalysts. The dispersion of copper species and the metal–support interaction were comprehensively studied by means of TPR, XRD, cyclic voltammetry and XPS techniques. The catalytic activities for CO oxidation of CuO/CeO₂ catalysts were also compared.

2. Experimental

2.1. Catalyst preparation

The CeO₂ powder was prepared by precipitation of Ce (NO₃)₃·6H₂O aqueous solution with the addition of NH₃·H₂O solution until the pH of the mixed solution greater than 9.0 under vigorous stirring at 60 °C. The precipitant was then aged in the mother liquid for 4 h, followed by filtration and washing with distilled water. The obtained solid was dried at 100 °C for 10 h, and calcined at 450 °C for 4 h in air. Copper oxide was then loaded on the prepared CeO₂ power by two ways. (1) Impregnation: CeO₂ support was impregnated with an aqueous solution of Cu (OAc)₂·H₂O for 24 h; excess water was then vaporized at 70 °C by heating, followed by drying at 100 °C for 10 h and calcined at 450 °C for 4 h in air. The catalyst thus obtained was designed as CuO/CeO₂ (imp). (2) Deposition-precipitation: the CeO₂ powder was first suspended in the aqueous solution of appropriate amount of Cu (OAc)₂·H₂O. Then, a 0.25 M Na₂CO₃ solution was gradually added to the suspended solution containing CeO₂ and copper precursor until the pH of the mixed solution reached to 9.0 and further aged for 1 h under vigorous stirring at 70 °C during which copper hydroxide was exclusively precipitated on the surface of CeO₂. The resulting solid was washed with hot distilled water, dried at 100 °C for 10 h, and subsequently calcined in air at 450 °C for 4 h. The catalyst thus obtained was referred as CuO/CeO₂ (DP).

For comparison, a CuO/CeO₂ catalyst was prepared by co-precipitation. Aqueous solution of Cu(OAc)₂·H₂O and Ce(NO₃)₃·6H₂O was co-precipitated with equivalent quantity of Na₂CO₃ solution under vigorous stirring at 50 °C.

After aging for 2 h, the precipitate was filtered and thoroughly washed with hot distilled water. The precipitate was then dried at 100 °C for 10 h, and calcined at 450 °C for 4 h in air. This procedure gave the catalyst as CuO/CeO₂ (CP).

2.2. Characterization

Power X-ray diffraction (XRD) patterns were measured using a Rigaku D/MAX-RB with Cu K α radiation operated at 40 kV and 100 mA.

Temperature-programmed reduction (TPR) was carried out in a flow system at CHEMBET 3000 adsorption instrument (QuantaChrome Inc., US) equipped with a TCD detector. Sample of 100 mg CuO/CeO₂ was loaded and pretreated in He flow at 400 °C for 1 h to remove the adsorbed carbonates and hydrates. After cooling down to room temperature and introducing the reduction agent of 5% H₂/Ar, the temperature was programmed to rise at a ramp of 10 °C/min. After the preliminary TPR was recorded, the sample was further subjected to re-oxidation with 20% O₂/N₂ at room temperature (RT) or 300 °C for 30 min, then degassed at 400 °C in He flow for 30 min to remove the adsorbed oxygen species. Subsequently, further TPR performances were conducted after cooling down to room temperature.

The specific surface areas (*S*_{BET}) of the catalysts were calculated from a multipoint Braunauer–Emmett–Teller (BET) analysis of the nitrogen adsorption isotherms at 77 K recorded on a micrometrics ASAP 2000 instrument.

XPS analyses were performed on an ESCALAB MK-II spectrometer (VG Scientific Ltd., UK), using Al K α radiation (1486.6 eV) operating at an accelerating voltage of 12.5 kV. Charging effects were corrected by adjusting the C 1s peak to a position of 284.6 eV. The samples were pressed into thin discs and mounted on a sample rod placed in a pre-treatment chamber. The spectra of Cu 2p, Cu L₃VV, Ce 3d and O 1s levels were recorded.

Cyclic voltammetry measurements were conducted at ambient temperature with an EG&G Model 273A potentiostat/galvanostat using a three-electrode cell configuration. The working electrode was a thin layer of Nafion-bonded mixture cast on a glassy-carbon disk electrode by mixing carbon black (Vulcan XC-72R, Cabot Corp.; *S*_{BET} = 236.8 m² g^{−1}) with CuO/CeO₂ powder samples. Sodium sulfate (0.05 M) was used as the electrolyte solution. The counter electrode used was a Pt foil and a saturated calomel electrode (SCE) was employed as the reference electrode. Prior to the measurement, the electrolyte solution was degassed through bubbling with high pure nitrogen (99.999%). The electrodes were cycled from +1.2 to −1.0 V at 10 mV s^{−1} scan rate for three sweep cycles.

2.3. Catalytic activity measurements

CO oxidation reaction was carried out in a fixed bed microreactor with a feed composition of CO/O₂/He = 1/1/98 (vol.%). Two-hundred and fifty milligrams (40–60 mesh)

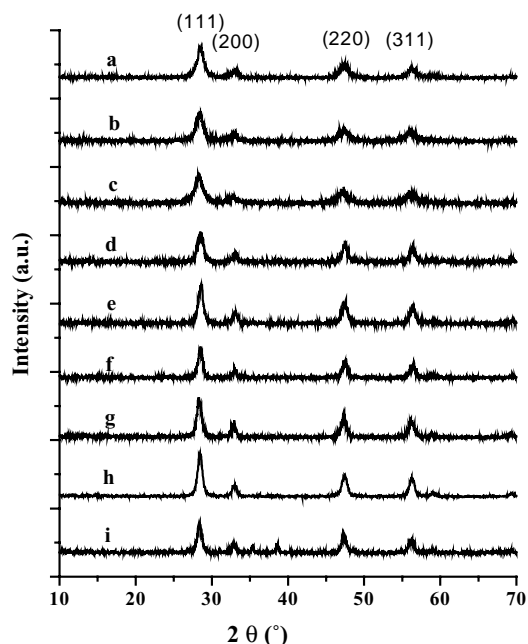


Fig. 1. XRD patterns of the CuO/CeO₂ samples: (a) 2.5 wt.% Cu (CP); (b) 5 wt.% Cu (CP); (c) 10 wt.% Cu (CP); (d) 2.5 wt.% Cu (DP); (e) 5 wt.% Cu (DP); (f) 10 wt.% Cu (DP); (g) 2.5 wt.% Cu (imp); (h) 5 wt.% Cu (imp); (i) 10 wt.% Cu (imp).

of CuO/CeO₂ catalysts was placed between two layers of quartz wool inside a quartz tube (i.d. = 6 mm) at atmospheric pressure. The reaction temperature ranged from 25 to 120 °C with a total feed gas flow rate of 43 ml/min, corresponding to a gas hourly space velocity (GHSV) of 10,000 h⁻¹. Effluents from the reactor were analyzed on line by a Varian 3800 gas chromatograph equipped with 13X molecular and Haysep D packing columns for the detection of CO, CO₂ and O₂ with He as the carrier gas.

3. Results and discussion

3.1. Surface area and XRD pattern

Fig. 1 shows the XRD patterns of CuO/CeO₂ catalysts containing 2.5–10 wt.% Cu prepared by impregnation,

deposition-precipitation and co-precipitation techniques. The distinct fluorite oxide diffraction pattern of CeO₂ was observed in all the cases. CuO phase giving strong reflections at 35.6° and 38.8° only appeared in the sample prepared by impregnation with copper loading of 10 wt.%. The absence of CuO diffraction in other samples may be that the copper particles are too small to be detected, and that copper particles well dispersed in the catalysts. Comparatively, the presence of CuO diffraction in CuO/CeO₂ (imp) with 10 wt.% copper loading should be ascribed to its heterodisperse of copper species and aggregation of part of copper species on the surface. Comparing with the catalysts prepared by deposition-precipitation and impregnation, the apparent broadening of the diffraction patterns of ceria in CuO/CeO₂ (CP) was observed, indicating that the CeO₂ particle size of CuO/CeO₂ (CP) was smaller than that of CuO/CeO₂ (DP) and CuO/CeO₂ (imp) catalysts.

The calculated average ceria crystallite size and BET results are listed in Table 1. The presence of Cu favors the formation of smaller CeO₂ particles during co-precipitation. CuO/CeO₂ (CP) catalysts showed smaller ceria crystallite size with respect to the pure CeO₂ support, indicating that the addition of copper during co-precipitation process inhibits the crystal growth of ceria, in agreement with the result by Fu et al. [17,18]. No apparent growth of the ceria crystals appeared with the increase of copper loading. The variations of preparation methods led to large differences in average ceria crystallite size and BET surface area. The average crystallite sizes of ceria were 6.30, 9.71 and 10.41 nm in the CuO/CeO₂ (5 wt.% Cu) catalysts prepared by CP, DP and imp methods, respectively. Combining all the average ceria crystallite size data, it is reasonable to say that co-precipitation method is favorable to obtain smaller particle size of ceria. The BET surface area of the prepared CeO₂ support was measured to be 103.5 m² g⁻¹, and the deposition of copper caused an obvious decrease in the specific surface area to 85.5 m² g⁻¹, while the BET surface area decreased to 92.5 m² g⁻¹ for the 5 wt.% Cu catalyst (DP).

XRD indicated that the copper species were highly dispersed, but the impregnation method led to relatively poor dispersion comparing with the other two methods. The calculated BET results suggested that co-precipitation caused

Table 1
The physical properties of CuO/CeO₂ catalysts

Composition (wt.% Cu)	Crystallite size ^a (nm) (CeO ₂ (1 1 1))	BET surface area (m ² g ⁻¹)	Average pore diameter (nm)	Pore volume (cm ³ g ⁻¹)
CeO ₂ powder	7.64	103.2	6.46	0.17
2.5 (imp)	9.97	89.7	6.42	0.17
5.0 (imp)	10.41	85.5	5.87	0.13
10.0 (imp)	10.34	83.9	6.23	0.14
2.5 (DP)	9.62	96.7	6.85	0.16
5.0 (DP)	9.76	92.5	7.96	0.17
10.0 (DP)	9.41	91.2	7.65	0.15
2.5 (CP)	6.47	104.5	4.10	0.15
5.0 (CP)	6.30	111.3	3.58	0.14
10.0 (CP)	5.91	117.6	3.46	0.14

^a Calculation from the peak at 28.6° in the XRD pattern using the Scherrer equation.

the smallest average ceria crystallite size and largest surface area, indicating more uniform dispersion. Therefore, we can conclude that the dispersion of the copper species in the catalyst is strongly influenced by the preparation method.

3.2. H_2 -TPR

Temperature-programmed reduction has been used extensively to characterize the reducibility of CuO/CeO₂ catalysts [19]. As well known, CeO₂ alone has two reduction peaks at about 430 and 900 °C, which are ascribed to the reduction of surface and bulk oxygen of CeO₂, respectively. Meanwhile, CuO only has single reduction peak at about 280 °C. The H_2 -TPR profiles of the 5 wt.% Cu catalysts prepared by three methods are shown in Fig. 2. It can be seen that the reduction behaviors of ceria were dramatically changed by the addition of copper. The reduction peak of surface oxygen of CeO₂ shifted to low temperature, the peak at 430 °C disappeared, and that the peak near 900 °C corresponding to the reduction of bulk oxygen of CeO₂ remained unchanged. Regardless of the preparation method, CuO/CeO₂ catalysts all had reduction peaks below 200 °C. This is conceivable that the interaction occurring at interface between copper oxide and surface oxygen vacancies of ceria becomes strong enough, so the redox properties of CuO/CeO₂ catalysts are greatly promoted. Comparing with the catalysts prepared by deposition-precipitation and co-precipitation, the catalyst prepared by impregnation had more H_2 consumption peaks, this may be ascribed to more different types of copper species that exist on the surface of ceria, or metal particles relatively heterodispersed in the catalyst.

In order to highlight the reversible redox ability, the samples subjected to the preliminary TPR processes were further re-oxidized with 20 vol.% O₂/N₂ at RT or 300 °C, followed by another TPR measurement. The reduction peak temperature and corresponding hydrogen consumption are listed in Table 2. The TPR profiles of the samples after these re-oxidation treatments were greatly modified. Both the relative intensities and the positions of reduction peaks were significantly changed, and the major reduction peak of copper oxides gradually moved toward higher temperature. These results gave evidence that reduction/oxidation processes take place at room temperature and re-oxidation at RT even can make almost the majority of copper and surface Ce³⁺ be oxidized. The sample (CP) re-oxidation at RT had the smallest hydrogen consumption among the three catalysts. Considering that the catalyst prepared by co-precipitation disperses uniformly in whole catalyst, we can conclude that RT only oxidize copper species dispersed on the surface, whereas the oxidation of the copper species in the bulk phase needs higher temperature. The total hydrogen consumption after re-oxidation at 300 °C was higher than that re-oxidation at RT; this can be understood by considering that the re-oxidation treatment at 300 °C oxidizes not only surface CeO_{2-x} to CeO₂, but also bulk CeO_{2-x} on the vicinity of copper species, and thus more hydrogen is

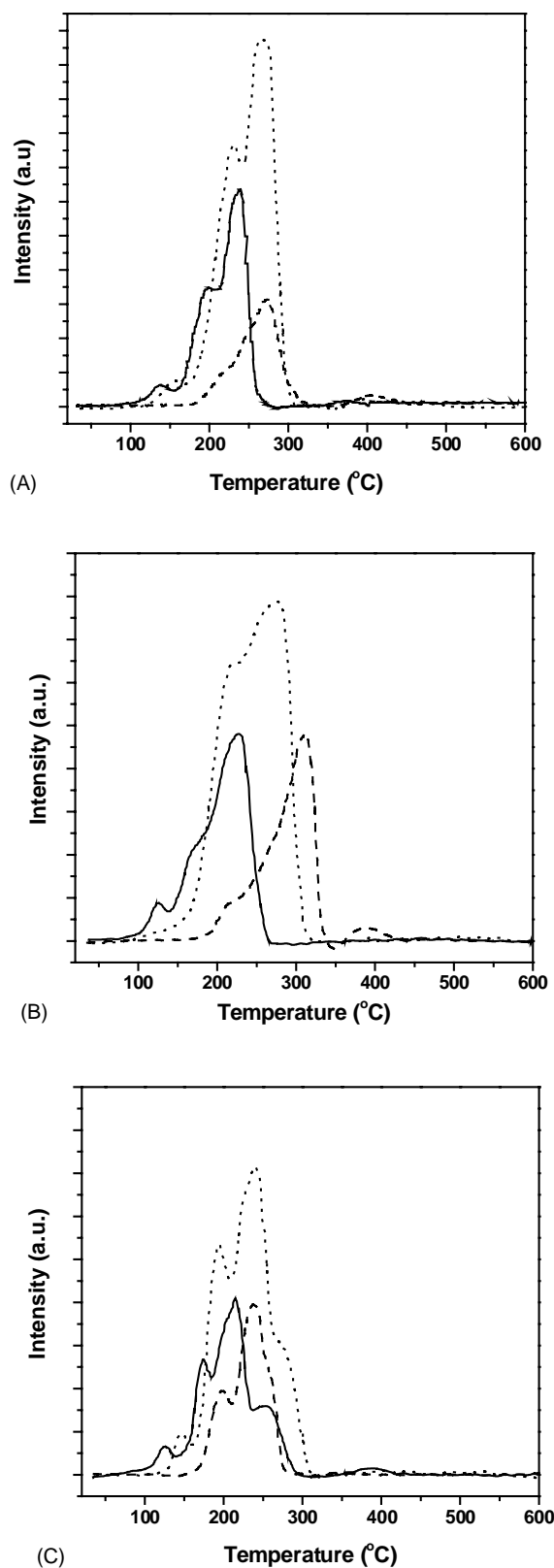


Fig. 2. The TPR profiles of CuO/CeO₂ catalysts (5 wt.% Cu): (A) CuO/CeO₂ (CP); (B) CuO/CeO₂ (DP); (C) CuO/CeO₂ (imp); (—) as-prepared; (---) re-oxidation at RT (···) re-oxidation at 300 °C.

Table 2
Comparison of reducibility and hydrogen consumption on CuO/CeO₂ (5 wt.% Cu) catalysts

Catalyst composition	H ₂ consumption ($\mu\text{mol/g}_{\text{cat}}$)				
	Peak 1 (T, °C)	Peak 2 (T, °C)	Peak 3 (T, °C)	Peak 4 (T, °C)	Peak 5 (T, °C)
CeO ₂	—	—	—	—	392.1 (433)
CuO/CeO ₂ (imp)	56.8 (128)	206.7 (173)	309.6 (211)	148.5 (258)	13.4 (387)
CuO/CeO ₂ (imp)-RT ^a	160.9 (195)	437.6 (237)	44.1 (262)	—	—
CuO/CeO ₂ (imp)-300 ^b	64.6 (148)	445.1 (191)	829.9 (236)	168.8 (283)	—
CuO/CeO ₂ (DP)	71.4 (122)	556.1 (187)	308.6 (226)	—	—
CuO/CeO ₂ (DP)-RT ^a	—	470.4 (269)	361.6 (309)	—	33.9 (393)
CuO/CeO ₂ (DP)-300 ^b	—	821.7 (229)	789.0 (278)	—	—
CuO/CeO ₂ (CP)	40.9 (137)	366.1 (201)	497.1 (237)	—	60.5 (384)
CuO/CeO ₂ (CP)-RT ^a	—	330.6 (249)	184.0 (274)	—	35.0 (407)
CuO/CeO ₂ (CP)-300 ^b	117.4 (155)	978.4 (231)	864.9 (270)	—	—

^a Re-oxidation at RT in 20% O₂/N₂.

^b Re-oxidation at 300 °C in 20% O₂/N₂.

consumed to reduce this part of ceria in the following TPR measurements. The total amount of hydrogen consumption of the CuO/CeO₂ (CP) sample re-oxidized at 300 °C exceeded that of the samples prepared by deposition-precipitation and impregnation methods, while the CuO/CeO₂ (imp) sample re-oxidized at 300 °C had the smallest hydrogen consumption. A possible explanation could be due to the difference of interaction between copper species and ceria. The CuO/CeO₂ (CP) sample had the strongest metal–support interaction. These results suggested that considerable changes in the morphology of the dispersed copper species occurred during the reduction–oxidation cycle.

According to above analysis, we can ascribe the first reduction peak to the reduction of CuO on the ceria surface, the second peak to the reduction of larger CuO species on the surface and the third peak (about 280 °C) to the reduction of bulk CuO and surface CeO₂. The fourth peak (about 450 °C) was very small and can be assigned to the reduction of residual CeO₂ on the surface. Noticeably, it can be found that the total amount of hydrogen consumption depended strongly on the re-oxidation temperature and preparation methods.

Fig. 3 shows the TPR profiles of CuO/CeO₂ (CP) catalysts with different copper loading. With the increase of copper loading, the temperature of reduction peak initially shifted to lower temperature and then increased. When the copper loading was very low, the temperature of reduction peak of CuO/CeO₂ (CP) catalysts only slightly decreased comparing with that of pure ceria. Take 0.5 wt.% Cu as example, the temperature of reduction peak was 380 °C, indicating that the reduction behavior of ceria only be slightly changed by a small amount of copper species. Once the copper loading located in the range of 2.5–10 wt.%, the temperature of reduction peaks of copper species and surface ceria all dramatically decreased to below 200 °C and the TPR profiles showed multi-reduction peaks. In all the catalysts prepared by co-precipitation, the 10 wt.% Cu sample had the largest hydrogen consumption (360.2 $\mu\text{mol/g}_{\text{cat}}$) at low temperature (131 °C), indicating more easily reduced

copper particles dispersed on the surface of ceria. Further increasing copper loading, the H₂ consumption peak shifted to high-temperature region. Noticeably, when copper loading exceeded 20 wt.%, only one broad reduction peak existed at about 240 °C and a shoulder peak presented at the side of low temperature; this may suggest the relatively uniform distribution of larger copper particle or copper oxide clusters in connection with ceria that exist in these catalysts. When copper loading attains a certain value, copper species have more chances to aggregation through collision during precipitation procedure. So this remarkable change of the TPR profiles can be due to the aggregation of small copper species into larger bulk particles of copper in preparation process, and the relatively larger copper oxide clusters are more difficult to be reduced.

TPR results convincingly evidenced that the addition of copper significantly improved the reducibility of the ceria,

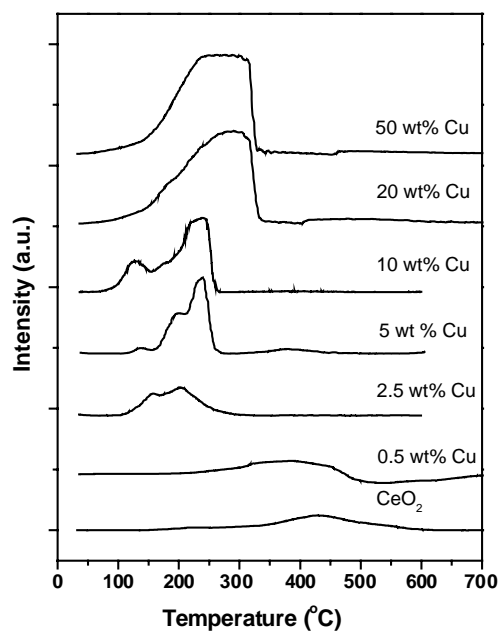


Fig. 3. The TPR profiles of CuO/CeO₂ catalysts (CP) with different copper loading.

especially ceria in vicinity of copper species. Simultaneously, the presence of ceria also promoted the reduction of copper. The CuO/CeO₂ catalyst (CP) has more excellent redox properties and stronger metal–support interaction in three CuO/CeO₂ catalysts. The amount of surface oxygen available for reduction is controlled by the crystal size of ceria and dispersion of copper species.

3.3. Cyclic voltammetry

Since cycle voltammetry test can provide convincing evidences for the redox ability of redox couples during the oxidation and reduction procedures [20], it seems possible to apply this technique to further investigate the reversible redox ability of the present CuO/CeO₂ catalysts. The difference in the redox ability of CuO/CeO₂ catalysts prepared by different preparation routes is shown in Fig. 4. The sample prepared by co-precipitation had the highest reversible redox ability among the three catalysts, showed reduction and oxidation peaks at -0.06 and $+0.027$ V, respectively. In contrast, the sample (DP) exhibited reduction and oxidation peaks at -0.11 and $+0.035$ V, while the sample (imp) presented reduction and oxidation peaks at -0.11 and $+0.063$ V, indicating that copper species in the CuO/CeO₂ catalysts prepared by deposition-precipitation and impregnation methods required more energy to be reduced and oxidized. This result reflects the discrepancy in the degree of interaction, which leads to variation in redox properties. Stronger interaction between copper species and ceria in CuO/CeO₂ (CP) catalyst leads to the most excellent redox ability. In addition, for the sample prepared by co-precipitation and deposition-precipitation, the reduction potential in the second sweep for CuO/CeO₂ catalyst shifted to higher value, and the oxidation potential shifted to lower value, indicating that electronic redox cycle leads to the improvement of redox ability. In contrast, the CuO/CeO₂ (imp) sample did not show this change, implying weaker

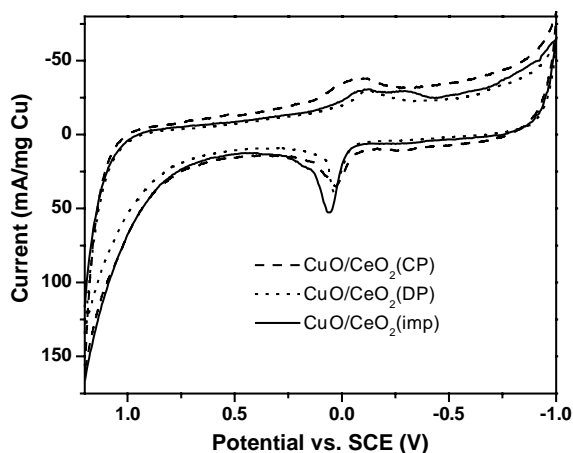


Fig. 4. Cyclic voltammograms of copper species in CuO/CeO₂ catalysts (5 wt.% Cu) (50 ml/min 5% H₂/N₂) in 0.05 M Na₂SO₄ electrolyte at a scan rate of 10 mV s⁻¹.

Table 3

XPS data measured for the CuO/CeO₂ (5 wt.% Cu) prepared by different methods

Preparation method	Atomic ratio		Ce (III) (%)	O _{lat} (%)
	Cu/Ce	Ce/O		
imp	0.3920	0.2099	24.3	24.1
DP	0.3889	0.2187	22.1	24.7
CP	0.2549	0.3163	26.4	26.9

metal–support interaction. This result agrees well with TPR results, indicating the variation of redox ability originated from different preparation methods.

3.4. X-ray photoelectron spectroscopy

Comparing XPS spectra of Cu L₃VV Auger and Cu 2p, we found all CuO/CeO₂ (5 wt.% Cu) catalysts showed slightly reduced copper phase, part of Cu⁺ existed in the as-prepared catalysts. This could be mainly due to the slight photoreduction of CuO in the spectrometer. The atomic surface compositions and the %Ce(III) of the catalysts are shown in Table 3. A favorable method which considers the relative intensity of the u_0 (v_0) and u' (v') peaks to the intensity of Ce 3d region was applied to estimate the reduction degrees of ceria [21]. In three catalysts, the reduction degree of ceria was very close, but the sample (5 wt.% Cu) prepared by co-precipitation had the highest Ce(III) % value (about 26.4%). Table 3 further demonstrated the surface atomic compositions that depend on the preparation method. Obviously, the sample (imp) had more copper species dispersed on the surface than the other catalysts, indicated by a higher Cu/Ce atomic ratio value. This represented a quantitative evolution of the dispersion properties of the copper species at the ceria surface. Fig. 5 shows the O 1s spectra for CuO/CeO₂ catalysts. In addition to the

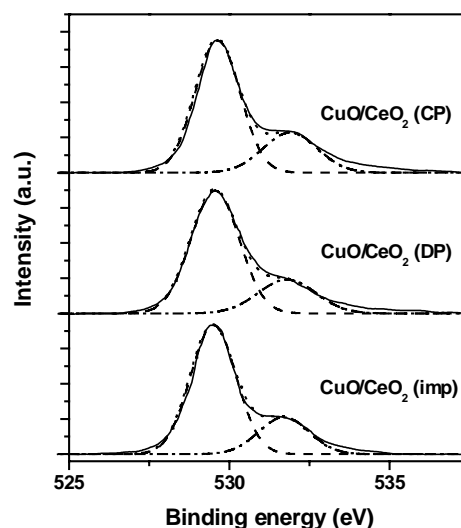


Fig. 5. XPS spectra of O 1s for CuO/CeO₂ catalysts prepared by different methods.

presence of the main peak at 529.5 eV, an apparent shoulder peak appeared at 532.4 eV, representing the existence of lattice oxygen vacancies. Holgado et al. attributed this O_{lat} peak to such highly polarized oxide ions at the surface (and interfaces) of the nanocrystallites with an unusual low coordination [15]. The CuO/CeO₂ (CP) had the relatively higher intensity of O_{lat} peak (% O_{lat} is 26.9) in three catalysts with same copper loading, suggesting the existence of more lattice oxygen vacancies. The quantitative estimation with regard to the total area of the peak is shown in Table 3.

XPS measurement showed copper species enriched on the surface of the catalysts prepared by deposition-precipitation and impregnation methods. Combining the XRD and BET results, we can conclude that the metal–support interaction depends on the dispersion of metal. The stronger the interaction between copper and ceria, the easier the redox process. Uniform dispersion can lead to stronger interaction between dispersed copper species and ceria, which is responsible for the improvement of redox properties of the CuO/CeO₂ catalysts.

3.5. Activity measurements

The effect of copper loading of the CuO/CeO₂ catalysts prepared with various methods on CO oxidation activity is presented in Fig. 6. Among the catalysts prepared by deposition-precipitation and impregnation, 5 wt.% Cu sample showed higher activity comparing with 2.5 and 10 wt.% Cu samples, but for the catalysts prepared by co-precipitation, the catalytic activity of CO oxidation increased with the copper loading from 2.5 to 10 wt.%. The 10 wt.% Cu (CP) catalyst showed the highest activity, and obtained complete CO conversion at 85 °C.

Addition of copper significantly reduced the temperature of complete oxidation, and all CuO/CeO₂ catalysts showed good catalytic activity for CO oxidation. Comparatively, the CuO/CeO₂ (CP) catalyst presents the highest catalytic activity for CO oxidation in three catalysts with same copper loading (5 wt.%), the complete oxidation temperature of the CuO/CeO₂ (CP) was lower than that of the corresponding catalysts prepared by deposition-precipitation and impregnation methods, and gave almost complete CO conversion at 100 °C. The catalysts prepared by deposition-precipitation and impregnation method presented similar activity, but CuO/CeO₂ (DP) catalyst presented slightly better catalytic activity than CuO/CeO₂ (imp) catalyst.

Considering the features of different preparation methods, the differences of redox properties and catalytic activities may originate from the variation of distribution of copper species. Co-precipitation method caused copper species uniformly dispersed in whole bulk phase, and the catalyst had the smallest average ceria crystallite size and the largest surface area. These features evidence larger interface between copper species and ceria, resulting in strong metal–support interaction. In contrast with the catalyst prepared by co-precipitation, the catalysts prepared by

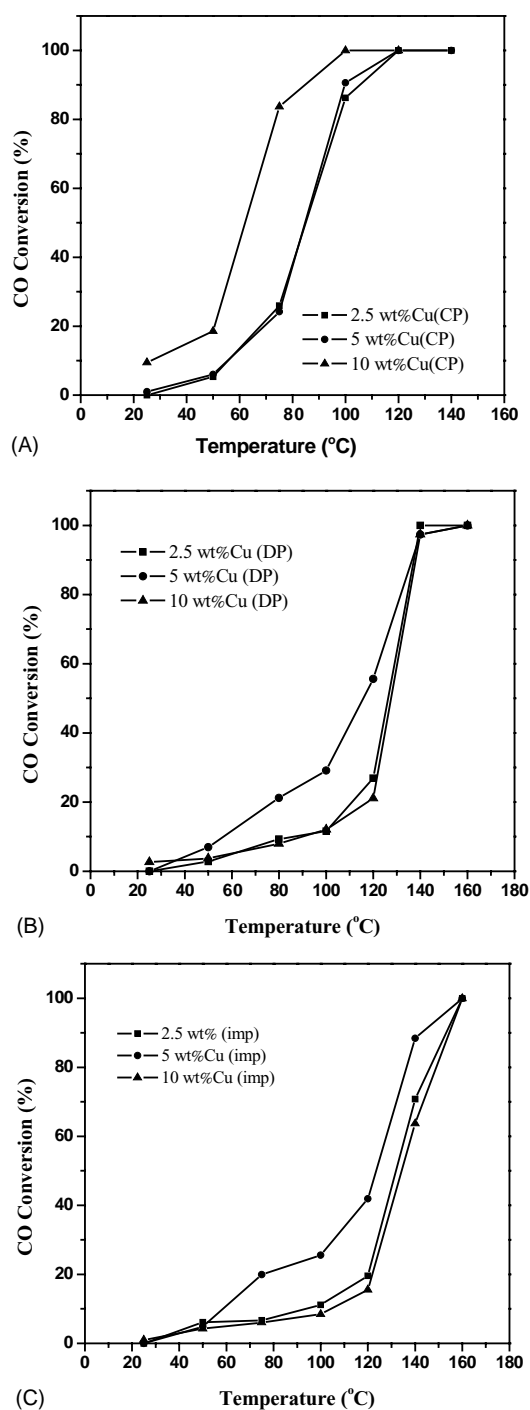


Fig. 6. Effect of copper loading on the CO oxidation for CuO/CeO₂ catalysts prepared by (A) co-precipitation; (B) deposition-precipitation; (C) impregnation; (■) 2.5 wt.% Cu; (●) 5 wt.% Cu; (▲) 10 wt.% Cu.

deposition-precipitation and impregnation methods exhibited larger average ceria crystallite size, and copper species enriched on the surface of these two catalysts. Therefore, it can be expected that a less interface area between copper species and ceria produce relatively weaker metal–support interaction. In addition, it must be noted that a difference between the CuO/CeO₂ (DP) and the CuO/CeO₂ (imp) catalyst is the dispersion of copper species on the surface,

but presents more uniform dispersion for the former. This could be interpreted as the aggregation of copper species in vaporization process for the CuO/CeO₂ (imp) catalyst. The appearance of the larger copper particles further minimizes the interface area, thus the metal–support interaction is weakened. These results suggested that preparation routes govern the metal–support interaction. In addition, the CuO/CeO₂ (CP) had the relatively higher intensity of O_{lat} peak in three catalysts with 5 wt.% copper loading, suggesting more lattice oxygen vacancies.

Based on the above results, we can conclude that the catalytic activity is related to the copper loading and preparation route. All catalysts showed good catalytic activity for CO oxidation reaction, which can be ascribed to the enhancement of the redox properties. This suggests that the strong interaction between copper and ceria is responsible for the enhancement of the low temperature activity of CO oxidation reaction. That is to say, the strongest metal–support interaction exists in the catalyst prepared by co-precipitation among the three catalysts.

4. Conclusions

A series of CuO/CeO₂ catalysts prepared by three different preparation methods were investigated. The correlations between catalytic activity and redox properties or preparation method were obtained.

The catalytic activity of CuO/CeO₂ catalysts strongly depends on preparation route and metal loading. The catalysts prepared by co-precipitation methods showed the best catalytic activity, this is ascribed to uniform dispersion and strong interaction between copper species and ceria. The changes of the degree of interaction can strongly affect the redox properties of supported copper catalysts, producing significant differences in catalytic performance for CO

oxidation reaction. The stronger the interaction between copper and ceria, the easier the redox process.

References

- [1] P. Zimmer, A. Tschöpe, R. Birringer, *J. Catal.* 205 (2002) 339.
- [2] J.B. Wang, D.H. Tsai, T.J. Huang, *J. Catal.* 208 (2002) 370.
- [3] P. Praserthdam, T. Majitnapakul, *Appl. Catal.* 29 (1994) 108.
- [4] W. Liu, M. Flytzani-Stephanopoulos, *J. Catal.* 153 (1995) 304.
- [5] P. Knauth, G. Schwitzgebel, A. Tschöpe, S. Villain, *J. Solid State Chem.* 140 (1998) 295.
- [6] A. Trovarelli, *Catal. Rev.* 38 (1996) 439.
- [7] J.B. Wang, W.H. Shih, T.J. Huang, *Appl. Catal. A* 203 (2000) 191.
- [8] B. Skårman, D. Grandjean, R.E. Benfield, A. Hinz, A. Andersson, L.R. Wallenberg, *J. Catal.* 211 (2002) 119.
- [9] Y.Y. Liu, H. Takashi, *Appl. Catal. A* 223 (2002) 137.
- [10] J.Y. Liu, J.L. Shi, D.H. He, Q.J. Zhang, X.H. Wu, Y. Liang, Q.M. Zhu, *Appl. Catal. A* 216 (2001) 113.
- [11] S.M. Zhang, W.P. Huang, X.H. Qiu, *Catal. Lett.* 80 (2002) 41.
- [12] B. Skårman, T. Nakayama, D. Grandjean, *Chem. Mater.* 24 (2002) 3686.
- [13] P.G. Harrison, I.K. Bull, W. Azalee, W. Daniell, D. Goldfarb, *Chem. Mater.* 12 (2000) 3715.
- [14] S. Bernal, J.J. Calvino, M.A. Cauqui, J.A. Pérez Omil, J.M. Pintado, J.M. Rodríguez-Izquierdo, *Appl. Catal. B* 16 (1998) 127.
- [15] J.P. Holgado, G. Munuera, J.P. Espinós, A.R. González-Elipe, *Appl. Surf. Sci.* 158 (2000) 164.
- [16] A. Martínez-Arias, M. Fernández-García, O. Gálvez, J.M. Coronado, J.C.A. Anderson, J. Cataluña, R. Conesa, J.C. Soria, G. Munuera, *J. Catal.* 195 (2000) 207.
- [17] J.B. Dow, T.J. Huang, *J. Catal.* 100 (1996) 171.
- [18] Q. Fu, W. Adam, M. Flytzani-Stephanopoulos, *Catal. Lett.* 77 (2001) 87.
- [19] A. James, B. McNicol, *Temperature-programmed reduction for solid materials characterization*, Dekker, New York, 1986.
- [20] P. Bera, S. Mirea, S. Sampath, M.S. Hegde, *Chem. Commun.* 927 (2001).
- [21] J. Silvestre-Albero, F. Rodríguez-Reinose, A. Sepúlveda-Escribano, *J. Catal.* 210 (2002) 127.